AD-A062 951 CALIFORNIA UNIV SANTA BARBARA QUANTUM INST F/G 7/3
HOW CARBON MONOXIDE BONDS TO ALUMINA-SUPPORTED RHODIUM PARTICLE--ETC(U)
NOV 78 R M KROEKER, W C KASKA, P K HANSMA N00014-78-C-0011
UNCLASSIFIED TR-1 NL

/ OF /
AD
AO 62951

END
DATE FILMED
3-79
DDC

LEVEL II

(12)

OFFICE OF NAVAL RESEARCH

(15) Contract N00014-78-C-0011

NR 056-673/11-18-77 (472)

(9) TECHNICAL REPORT NO. 1

(6) How Carbon Monoxide Bonds to Alumina-Supported Rhodium Particles: Tunneling Spectroscopy Measurements with Isotopes.

by

(70) R.M. Kroeker, W.C. Kaska and P.K. Hansma

Prepared for publication

in the

Journal of Catalysis

(14) TR-1

Quantum Institute
University of California
Santa Barbara, CA

(12) 25p.

(11) November 1978

407 624

Unclassified

SECURITY CLASSIFICATION OF THIS PAGE (When Data Entered)

REPORT DOCUMENTATION PAGE		READ INSTRUCTIONS BEFORE COMPLETING FORM
1. REPORT NUMBER: No. 1	2. GOVT ACCESSION NO.	3. RECIPIENT'S CATALOG NUMBER
4. TITLE (and Subtitle): HOW CARBON MONOXIDE BONDS TO ALUMINA-SUPPORTED RHODIUM PARTICLES: TUNNELING SPECTROSCOPY MEASUREMENTS WITH ISOTOPES		5. TYPE OF REPORT & PERIOD COVERED: Technical Report 6. PERFORMING ORG. REPORT NUMBER
7. AUTHOR(s): R.M. Kroeker, W.C. Kaska, P.K. Hansma		8. CONTRACT OR GRANT NUMBER(s): N00014-78-C-0011
9. PERFORMING ORGANIZATION NAME AND ADDRESS: Quantum Institute, University of California, Santa Barbara, California 93106		10. PROGRAM ELEMENT, PROJECT, TASK AREA & WORK UNIT NUMBERS: 121309
11. CONTROLLING OFFICE NAME AND ADDRESS: Office of Naval Research - Dept. of Navy, 800 N. Quincy St., Washington, D.C. 22217		12. REPORT DATE: November 1978 13. NUMBER OF PAGES: 24
14. MONITORING AGENCY NAME & ADDRESS (if different from Controlling Office): Office of Naval Research Branch Office, 1030 E. Green St., Pasadena, California 91101		15. SECURITY CLASS. (of this report): Unclassified 15a. DECLASSIFICATION/DOWNGRADING SCHEDULE

16. DISTRIBUTION STATEMENT (of this Report)

This document has been approved for public release and sale; its distribution is unlimited.

17. DISTRIBUTION STATEMENT (of the abstract entered in Block 20, if different from Report)

18. SUPPLEMENTARY NOTES

Accepted for publication in the Journal of Catalysis.

19. KEY WORDS (Continue on reverse side if necessary and identify by block number)

Fischer-Tropsch, methanation, supported metal catalysts, inelastic electron tunneling spectroscopy

79 01 05 038

20. ABSTRACT (Continue on reverse side if necessary and identify by block number)

Carbon monoxide chemisorbs in at least three different ways on alumina-supported rhodium particles: There are two different linear-bonded species and at least one bridge-bonded species. These conclusions from tunneling measurements on a model catalyst surface are based on isotope shifts with ^{13}CO and $C^{18}O$. They are in agreement with the conclusions from infrared measurements on dispersed metal catalysts.

C(18)O C(18)O

DD FORM 1 JAN 73 1473 EDITION OF 1 NOV 65 IS OBSOLETE

Unclassified

SECURITY CLASSIFICATION OF THIS PAGE (When Data Entered)

How Carbon Monoxide Bonds to Alumina-Supported Rhodium Particles: Tunneling Spectroscopy Measurements with Isotopes*

R. M. Kroeker, W. C. Kaska, and P. K. Hansma†

Department of Physics (RK & PH) and Department of Chemistry (WK)

University of California, Santa Barbara, CA 93106

ABSTRACT

Carbon monoxide chemisorbs in at least three different ways on alumina-supported rhodium particles: There are two different linear-bonded species and at least one bridge-bonded species. These conclusions from tunneling measurements on a model catalyst surface are based on isotope shifts with ^{13}CO and $C^{18}O$. They are in agreement with the conclusions from infrared measurements on dispersed metal catalysts.

*This work was supported in part by the Office of Naval Research. and by National Science Foundation Grant DMR76-83423.

†Alfred P. Sloan Foundation Fellow.

I. INTRODUCTION

Several methods for obtaining vibrational information of surface species have been developed. The oldest, infrared spectroscopy, has been joined by electron energy loss spectroscopy, inelastic neutron scattering, and inelastic electron tunneling spectroscopy.[1] The types of surfaces studied by these four techniques differ widely, from the ultraclean crystals studied by electron energy loss spectroscopy to the commercial catalysts that can be studied with infrared spectroscopy.[2]

This paper is an extension of a previously reported tunneling spectroscopy study[3] of a well characterized model system that closely resembles supported metal catalysts: It consists of small rhodium particles on alumina. The alumina support is obtained by oxidizing an evaporated thin aluminum film. Its properties closely resemble those of γ-alumina.[4] Rhodium is evaporated onto this alumina, where it forms highly dispersed small particles. See Figure 1. These 30Å particles are of similar size and distribution as those formed from the reduction of transition metal salts on alumina to form commercial catalysts.[5]

This similarity between our model catalyst and those of infrared spectroscopy workers, such as Yang and Garland,[6] permits direct comparison of tunneling data with published infrared data. From this comparison we conclude that the surface species are the same for our model system as for a dispersed metal catalyst. We also make an estimate of the dipole derivative for the adsorbed species from the observed peak shifts between tunneling and infrared data.

II. EXPERIMENTAL METHODS

The details of the preparation of inelastic electron tunneling spectroscopy tunneling junctions have been reported elsewhere.[7] A brief description of the procedure follows.

Aluminum electrodes are deposited in high vacuum onto a glass slide. These thin aluminum films, usually 800Å thick, are oxidized at 200°C in air to form the alumina insulating barrier necessary for tunneling. The oxidized electrodes are cleaned in an argon glow discharge prior to the deposition of rhodium. The rhodium is evaporated either in the presence of carbon monoxide or in high vacuum, followed by exposure to CO. A CO pressure of 1×10^{-5} torr is sufficient to dominate the residual gases present, typically 1×10^{-7} torr H_2O and H_2, and is maintained in the system to achieve a total exposure of typically 10^3 Langmuirs. Junctions are then completed by the evaporation of the top lead electrode. In this work all doped junctions were formed adjacent to undoped, control junctions to allow the subtraction of background structure. The differential spectrometer used has been described in the literature.[8]

Isotopically labeled CO was obtained from Stohler isotopes ($^{12}C^{18}O$) and Merck, Sharp and Dohme ($^{13}C^{16}O$), and was used as received.

Peak positions were measured relative to the background slope and averaged for many samples, to enable the detection of shifts as small as 0.2 meV. An averaging procedure was necessary because the absolute peak positions of several modes varied as much as 0.4 meV from sample to sample. Peak shifts were measured between

differential spectra of equal rhodium coverage. Again, averages of measured shifts were taken. All position measurements were taken from spectra with an expanded voltage axis (10 mV per inch).

III. DATA

Figure one shows a transmission electron micrograph of our rhodium-alumina surface. The large crystalline structure is the polycrystalline aluminum film that serves as the bottom electrode. (The alumina is thin, on the order of 20 Å thick.) The deposited rhodium can be seen as small spots covering the entire photograph. The average particle size is near 25 Å. It should be noted that the coverage of rhodium particles is uniform. The total mass of the deposited rhodium as measured with a quartz crystal microbalance is equivalent to a 4 Å thick continuous layer. This coverage of rhodium was used in this work because it corresponds to maximum peak intensities with good resolution in the tunneling spectra. Higher rhodium coverages give increased overall peak intensities, but fail to resolve the two lowest modes.

The differential tunneling spectra of CO chemisorbed on rhodium is shown in Figure 2. The positions of peaks due to rhodium - CO have been indicated. The positions of these vibrations are tabulated in Table I for the three isotopes of CO used. Positions listed are averages, and sample standard deviations are given.

IV. INTERPRETATION

The isotope shifts for the vibrations at 215.2 and 242.7 meV (1721 and 1942 cm^{-1}) respectively, confirm that these modes are, as one expects, carbon oxygen stretching modes.[2] From studying

sample to sample variations in intensity, it was found that the amplitude of the mode at 242.7 meV was correlated with a linear combination of the amplitudes of the two lowest modes, 51.6 and 58.1 meV (413 and 465 cm^{-1}). The relative amplitude of these two lowest modes was found to depend both upon the amount of rhodium evaporated and the amount of exposure to CO. The 51.6 meV mode dominates at low Rh coverages, with the 58.1 meV mode gaining in relative intensity at higher coverages. The 58.1 meV mode is the stronger mode at low CO coverages. For samples with a saturation CO coverage, as in Fig. 2, the mode at 51.6 meV dominates. The amplitude of the mode at 215.2 meV was correlated with the amplitude of the mode at 75 meV (600 cm^{-1}). Spectra showing the growth of the various modes with increasing rhodium coverage have previously been published.[3] Both high frequency modes were broad, having widths on the order of 10 to 12 meV.

The shifts observed in the low frequency modes are seen to be consistently larger for $^{13}C^{16}O$ substitution than for $^{12}C^{18}O$ substitution. See Table I. Typical shifts for a metal carbon stretching vibration would be -0.6 meV for $^{13}C^{16}O$, and -1.2 meV for $^{12}C^{18}O$.[9] It is seen that no observed low frequency mode can be assigned to a metal carbon stretching vibration. Typical shifts for a metal carbon monoxide bending vibration would be -1.6 meV for $^{13}C^{16}O$ and -0.6 meV for $^{12}C^{18}O$.[9] This agreement with the observed shifts, in both magnitude and direction enable the identification of the modes at 51.6 meV and 58.1 meV as bending modes. The widths of both these modes, approximately 5 meV, are larger than the instrumental line width. Typical separations of the bending modes

from the stretching modes for linear metal-carbon monoxide bonds are 2-3 meV.[9] This would place the corresponding stretching modes within the widths of the observed bending modes. Since the observed modes shift as bending modes, the stretching modes must be of relatively low intensity. The separation of these two bending modes, 6.5 meV, is much larger than the separation that might be expected for the degenerate bending modes of $Rh(CO)_2$. Thus, the identification of two bending modes indicates the presence of two types of linearly bonded CO molecules.

The mode at 75 meV involves both carbon and oxygen. The isotope shift data suggests it has a bending nature, but is not conclusive. As it is higher in frequency than the (linear) terminal modes, it is identified as at least one bridging species of CO. This mode showed the highest variability in position and shape, and thus has the largest uncertainty in the measured shift data.

The interpretation of the spectra of Figure 2 is then in terms of at least three species of CO: Two similar linearly bonded molecules with non-equivalent metal carbon bond strengths that exhibit bending vibrations at 51.6 meV and 58.1 meV. The corresponding stretching vibration of the carbon oxygen bond for both species appears as a broad band at 242.7 meV. In addition, at least one bridging species of CO can be seen at 75 meV and 215.2 meV.

The interpretation of the mode at 242.7 meV as being the superposition of the CO stretching modes of both linear species is supported by Figure 3. This figure is of a sample that has been heated to 150°C. The bending mode at 51.6 meV (413 cm^{-1}) in Figure 2 now appears greatly reduced in amplitude at 50.6 meV

(406 cm^{-1}). The bending mode at 58.1 meV (469 cm^{-1}) has shifted to 59.8 meV (478 cm^{-1}) and is nearly unchanged in amplitude. This gives additional support to our identification of the modes at 51.6 and 58.1 meV as due to different species. Note that the mode at 242.7 meV (1942 cm^{-1}) has shifted to 242.1 meV (1937 cm^{-1}) and also has been reduced in amplitude as would be expected if it originally contained unresolved contributions from the two species with different bending modes.

It must be emphasized, however, that our assignments of the peaks at 58.1 and 59.8 meV as bending modes means only that the shifts of these peaks with isotopes suggests that the dominant contribution is from bending modes. At the very least they contain some contribution from stretching modes as discussed above. They may also contain contributions from dissociated CO molecules as suggested by de Cheveigne et al. for their samples.

Note that in both Figures 2 and 3 an OH vibration is present. A straightforward interpretation is that the background water vapor bonds to the CO saturated rhodium particles. The implication is that there are sites available for hydroxyl groups that are not poisoned by exposure to CO.

It is apparent from Figure 3 that the reaction products contain C-H bonds. We are actively working to identify the products under different reaction conditions.

V. DISCUSSION

The results obtained above are in good agreement with those obtained by Yang and Garland[6] on alumina-supported rhodium. In their study a species consisting of two linear CO molecules bonded to a single rhodium atom, a linear species with one CO per rhodium atom, and a bridged species consisting of a CO bonded to two rhodium atoms, each of which also had a single linear CO were proposed.

Subsequent work by Garland, et al.,[10] on evaporated metal films of rhodium agreed with this interpretation, with the additional comment that a variety of bridged species seemed to exist that were sensitive to sample preparation. Their work also reported indications of weak adsorption in the spectral region of 575 to 400 cm^{-1} (72 to 50 meV); but spectrum quality did not allow identification of bands due to chemisorbed CO.

The results of Garland, et al.,[10] on evaporated rhodium films were confirmed by work done by Harrod, et al.[11] This work was done under ultra-high vacuum conditions; the CO used was not exposed to a hot rhodium filament.

A recent study on alumina supported rhodium by Arai and Tominaga[12] again confirmed the early results of Yang and Garland. In their work, the order of the metal-carbon bond strengths was determined by thermal desorption. Our assignment agrees with theirs; the bridging bond is the strongest (75 meV), the single linear species is the next strongest (58.1 meV), and the twin linear species has the weakest bond (51.6 meV).

Table II lists the reported positions of modes observed by several studies of CO on rhodium. The modes are labeled as to the species they are assigned to in the literature.

The variability of the bridging mode at 75 meV (600 cm^{-1}) of CO on rhodium that we have noticed is reflected by the presence of at least two types of bridging species in the infrared data; the mode at 1860 cm^{-1} (230.6 meV) reported by Arai and Tominaga,[12] and the mode at 1925 cm^{-1} (238.7 meV) reported by Yang and Garland.[6] These modes have been labeled (III)A, and (III)B, respectively, in Table II.

The twin linear species, labeled (I) in the table, has a doublet CO stretching vibration appearing at 2030 and 2100 cm^{-1} (251.7 and 260.4 meV). The single linear species, labeled (II) in Table II, has its CO stretching vibration at 2065 cm^{-1} (256 meV).

Comparison of the tunneling data with the infrared data shows:

1) Tunneling spectroscopy obtains vibrational information in the metal-carbon vibrational region. Intensities are strong, and the support gives negligible interference. This region was very useful for species identification.

2) The CO stretching modes are downshifted approximately 15 meV (120 cm^{-1}) and broadened relative to the infrared modes.

With the conclusion that the surface species in the tunneling junctions are the same as those in the infrared studies, the broadening and downshifting of the CO stretching vibration in the tunneling data is of interest. An essential difference between the infrared experiments and the tunneling experiments is the top

metal electrode in the tunneling experiments. Kirtley and Hansma[13] have studied the effect of the top metal electrode and found that it indeed produces broadening and downshifts by an image dipole effect. The broadening is found to be proporational to the downshift because of inequivalent sites. The downshift in frequency is:

$$\Delta\omega_{\perp} = \frac{-q_1^2}{32\pi\epsilon_o m\omega_o n_1^2 d^3}\left\{1 + \frac{3}{2}\sqrt{\frac{m\omega_o^2}{2E_D}}\frac{q_o d}{q_1}\left[1 - \left(1+\frac{a}{2d}\right)^{-2}\right]\right\} \qquad (1)$$

where aq_o and q_1 are the dipole moment and dipole derivative for the vibrational mode, ω_o is its frequency, m is its reduced mass, a is the bond length, E_D is the dissociation energy of the bond, n_1 is the dielectric constant of the oxide layer and d is the distance to the top lead electrode.

We can neglect the second term in the bracket since it is less than one even if $q_o \approx q_1$, and it is known for carbon monoxide and can be convincingly argued for metal carbonyls that $q_o << q_1$. We can approximate $n_1^2 d^3$ by the value found in fitting other peak shifts, 1.5×10^{-30} meter^3. We can use measured values for ω_o, ≈ 3.5 and $\approx 3.9 \times 10^{14}$ 1/sec for bridged and linear CO. We can calculate $m \simeq 1.14 \times 10^{-26}$ kg, leaving only q_1 unknown. Thus, if we assume the validity of Eq. (1), we can use it with our measured peak shifts, $\Delta\omega_{\perp} \approx 2.3 \times 10^{13}$ sec^{-1}, to estimate $q_1 \approx \sqrt{32\pi\epsilon_o m\omega_o (n_1^2 d^3)\Delta\omega_{\perp}} \approx 3.6 \times 10^{-19}$ coulomb $\approx$ 11 Debyes / Å.

For comparison Johnson and Lewis estimated[14] dipole derivatives in the range 9 to 15 Debyes/Å for various metal carbonyls from infrared intensity data. W. G. Rothschild kindly derived[15] an order of magnitude estimate of 18 Debyes / Å for Rh on γ-alumina[5a]

from infrared intensity data.[16] R. P. Eischens generously supplied us with integrated intensities from his published[17-19] and unpublished work that support the idea that the dipole derivative for CO adsorbed on supported metals is considerably larger than for free CO(3.1 Debyes/Å). His integrated peak intensities for chemisorbed CO are fifty to two hundred times larger than for gaseous CO. Though both our peak shift data and the infrared intensity data give only crude estimates of the dipole derivative, it is comforting that they are in the same ball park. At any rate, it shows that the peak shifts can be explained with physically reasonable parameters in the image dipole theory.[13]

However, recent careful work by H. Ibach[20] leads him to the conclusion that the dipole derivative for CO adsorbed on Pt was comparable to that for free CO. Perhaps there are fundamental differences between the situation for CO on Rh particles and CO on single crystal Pt. At any rate, we cannot explain the discrepancy.

A surprising feature of the data is the high intensity of the bending modes relative to the C-O stretching modes. We speculate that this is, at least partially, an orientation effect. The dominant contribution to the inelastic tunneling current is probably from tunneling electrons that pass near the edges of the cap-like particles (Fig. 1). Tunneling electrons that pass into the particles are unlikely to contribute.

Theory[21] and experiment[22] agree that tunneling electrons couple preferentially to vibrational modes with oscillating dipole moments parallel to the direction of tunneling. For CO molecules bonded to the edge of Rh particles perpendicular to the Rh surface,

the bending modes are parallel to the tunneling electrons. The CO stretching modes are then perpendicular to the direction of tunneling. Thus we would expect the bending modes to be enhanced relative to the CO stretching modes.

ACKNOWLEDGMENTS

We wish to thank S. de Cheveigne, R. P. Eischens, H. Ibach, V. G. Rothschild, and J. Schwarz for enlightening discussions. We wish to thank R. Gill for assistance in the use of the electron microscope.

REFERENCES

1. The first work in inelastic electron tunneling spectroscopy was done by: R. C. Jaklevic and J. Lambe, Phys. Rev. Lett. 17, 1139 (1967). Reference 7 is a recent review.
2. R. P. Eischens, Accts. Chem. Res. 5, 74 (1972), and references therein; J. Pritchard and T. Catterick, Experimental Methods in Catalytic Research, ed. R. B. Anderson and P. T. Dawson (Academic Press, 1976), Vol. III, p. 281.
3. P. K. Hansma, W. C, Kaska, and R. M. Laine, J. Am. Chem. Soc. 98, 6064 (1976).
4. P. K. Hansma, D. A. Hickson, and J. A. Schwarz, J. Catal. 48, 237 (1977).
5. a) Y. C. Yao, S. Japar, and M. Shelef, J. Catal. 50, 407 (1977). b) E. B. Prestridge, G. H. Via, and J. H. Sinfelt, J. Catal. 50, 115 (1977).
6. A. C. Yang and C. W. Garland, J. Phys. Chem. 61, 1504 (1957).
7. P. K. Hansma, Physics Reports 30, 145 (1977).
8. S. Colley and P. K. Hansma, Rev. Sci. Instrum. 48, 1192 (1977).
9. P. S. Braterman, Metal Carbonyl Spectra (Academic Press, New York, 1975), p. 25.
10. C. W. Garland, R. C. Lord, and P. F. Troiano, J. Phys. Chem. 69, 1188 (1965).
11. J. F. Harrod, R. W. Roberts, and E. F. Rissmann, J. Phys. Chem. 71, 343 (1967).
12. H. Arai and H. Tominga, J. Catal. 43, 131 (1976).
13. J. R. Kirtley and P. K. Hansma, Phys. Rev. B 13, 2910 (1976).
14. B. F. G. Johnson, J. Lewis, J. R. Miller, B. H. Robinson, and A. Wojciciki, J. Chem. Soc. (A) 522 (1968).

15. W. G. Rothschild, private communication.

16. H. C. Yao and W. G. Rothschild, J. Chem. Phys. 68, No. 11 (1978).

17. R. P. Eischens, Accts. Chem. Res. 5, 74 (1972).

18. D. M. Smith and R. P. Eischens, J. Phys. Chem. Solids 28, 2135 (1967).

19. D. J. Darensbourg and R. P. Eischens, Proc. Intl. Congr. Catalysis, Miami, Florida, 1972, paper #21 p. 371.

20. H. Ibach, Surf. Sci. 66, 56 (1977).

21. J. Kirtley, D. J. Scalapino, and P. K. Hansma, Phys. Rev. B 14, 3177 (1976).

22. J. T. Hall and P. K. Hansma, Surf. Sci. 71, 1 (1978).

FIGURE CAPTIONS

Fig. 1. Rhodium particles are shown in an electron micrograph of a specially prepared sample. The aluminum, evaporatively deposited and oxidized as in the preparation of a tunneling junction, is supported by a carbon coated nickel grid. The relatively large crystallites are in the aluminum metal film. The oxide on the aluminum metal is too thin to be seen. The rhodium particles appear as small hemispheres with a typical diameter of 25 Å.

Fig. 2. Differential spectra of carbon monoxide chemisorbed on alumina supported rhodium particles. Peaks labeled are modes studied with isotopes. Small peak at 116 meV (928 cm^{-1}) is due to the alumina support. (In earlier data,[3] an approximate correction for the effect of the superconducting energy gap of the Pb electrode was made by subtracting 6 cm^{-1} from observed peak positions.[13] Since this correction is only approximate for broad peaks, we have chosen not to make it here. Thus the reported peak positions are systematically higher here.)

Fig. 3. CO on rhodium on alumina heated to 150°C. One species of linear CO has reacted or thermal desorbed (406 cm^{-1}), while the second linear species remains (478 cm^{-1}). Note the bridged species (586 cm^{-1}) is also reduced in intensity. Isotopic labeling indicates the hydrocarbons formed are due to the CO chemisorbed on the rhodium particles. The large peak at 30 meV (240 cm^{-1}) is an instrumental effect. This peak, not shown in Fig. 2, is a subtraction error that is only present when the Pb electrode is superconducting. See Ref. 8.

TABLE I

$^{12}C^{16}O$	$^{13}C^{16}O$	Shift	$^{12}C^{18}O$	Shift
51.6 ± 0.2	49.9 ± 0.2	-1.7 ± 0.3	51.0 ± 0.2	-0.6 ± 0.3
58.1 ± 0.2	56.3 ± 0.2	-1.8 ± 0.3	57.4 ± 0.2	-0.7 ± 0.3
75.0 ± 1.0	73.0 ± 1.0	-2.0 ± 1.4	73.5 ± 1.0	-1.5 ± 1.4
215.2 ± 0.2	210.2 ± 0.2	-5.0 ± 0.3	210.4 ± 0.2	-4.8 ± 0.3
242.7 ± 0.3	238.2 ± 0.3	-4.5 ± 0.4	238.3 ± 0.3	-4.4 ± 0.4

Positions are measured in millielectron volts.

To convert to cm^{-1} multiply by 8.065.

TABLE II

Observed Mode Positions (cm^{-1})*

Yang and Garland[6]	Garland, et al.[10]	Harrod, et al.[11]	Aria and Tominaga[12]	Yao and Rothschild[16]	This Work
					413 I
	400-575				465 II
	'I','II','IIIA,B'				600 IIIA,B
					1721 IIIA,B
	1817	1820 IIIA,B			
	1852'IIIA'		1860 IIIA	1850 IIIA	
1925 IIIB	1905'IIIB'			1900 IIIB	1942 I,II
		2000 I,II		†2000 II	
2027 I			2040 I	2030 I	
2050 II	2055 II		2065 II		
2095 I	2111 I		2108 I	2100 I	

Species I 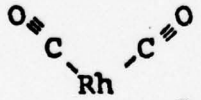

Species II 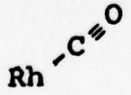

Species IIIA 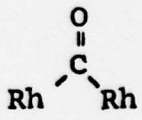

Species IIIB 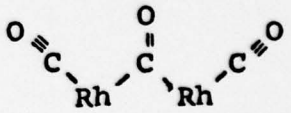

*To convert to meV, divide by 8.065

' ' Mode assignment is ours, not original authors'

†Observed in downshifted position after heating

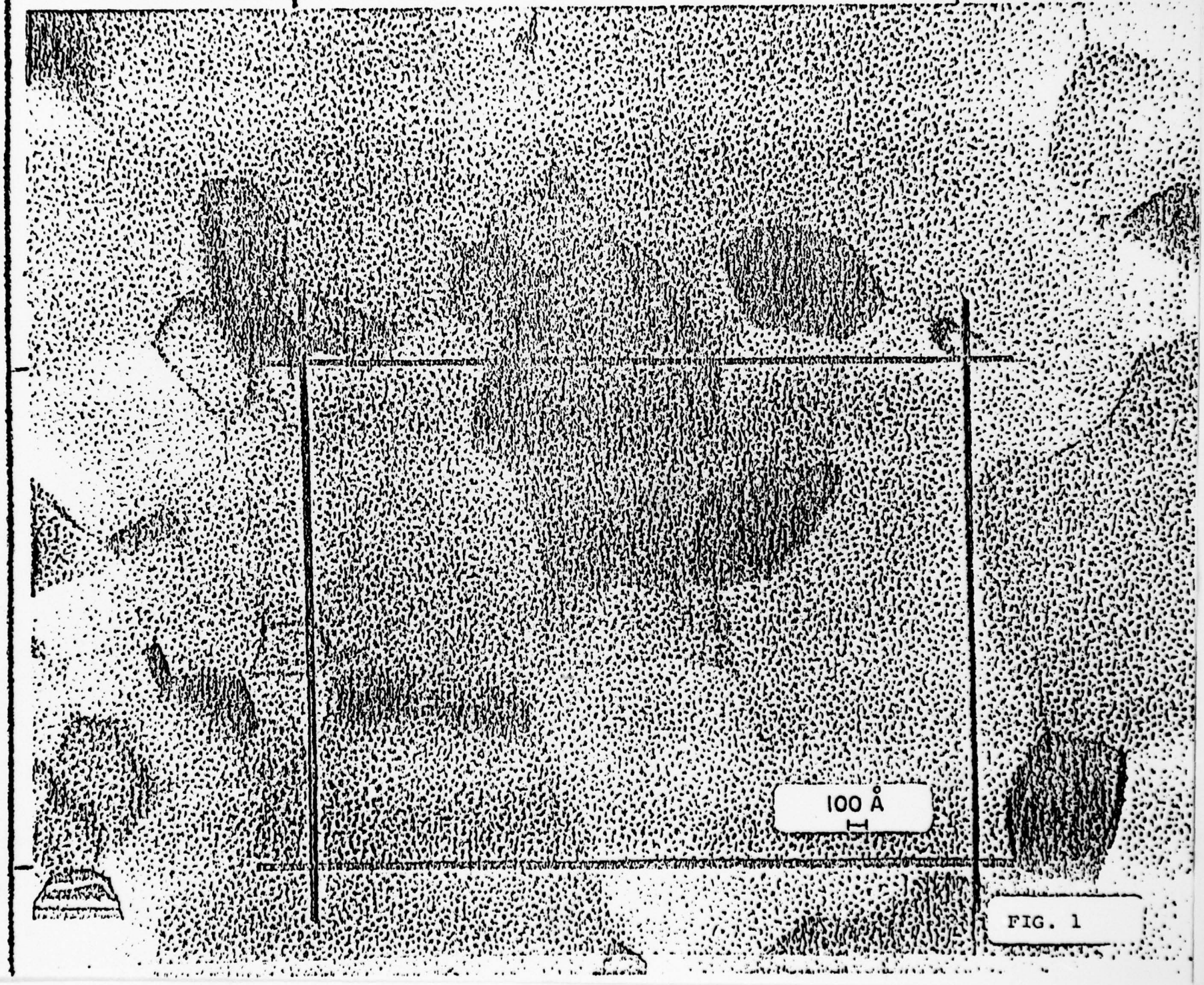

FIG. 1

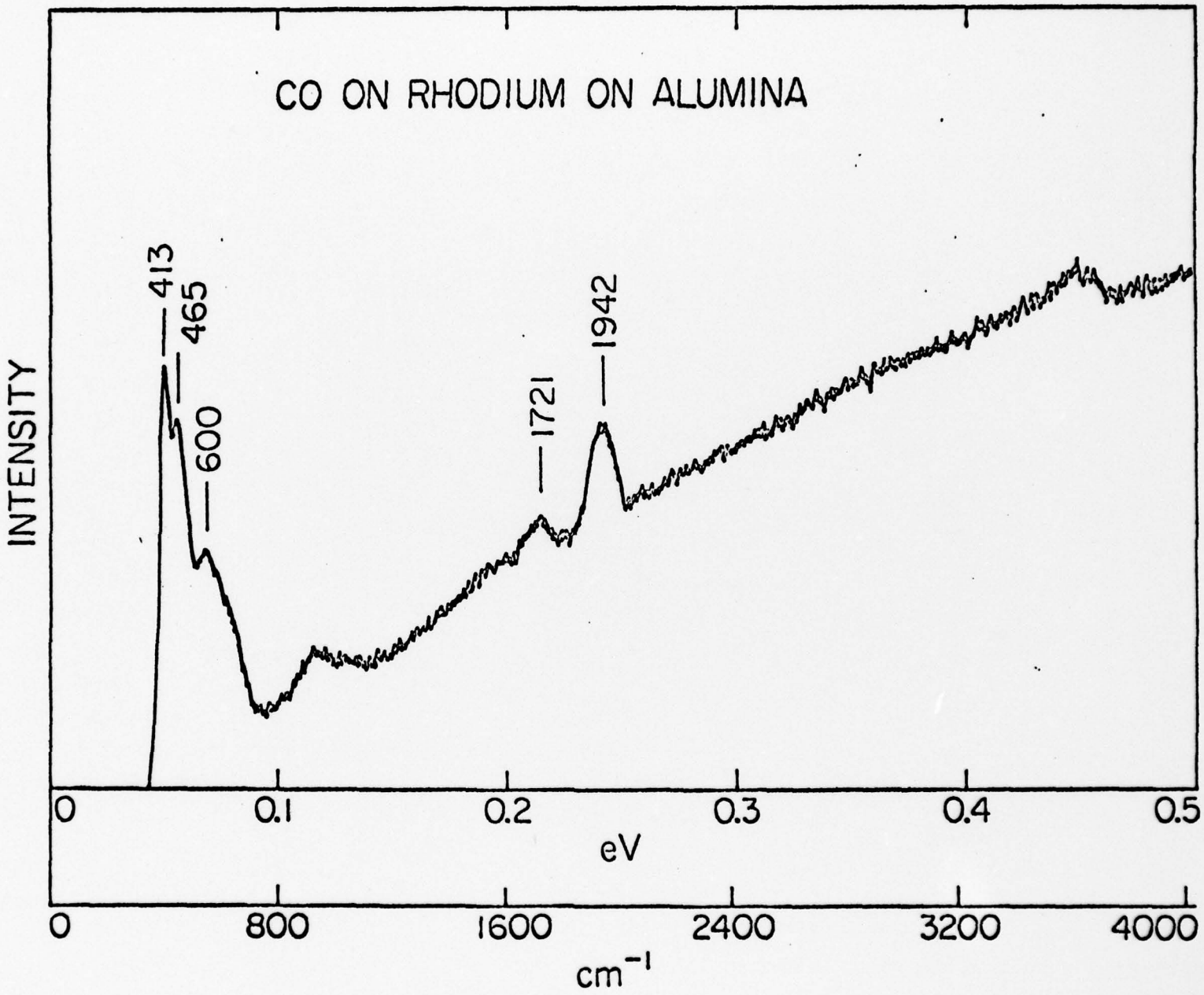
CO ON RHODIUM ON ALUMINA
INTENSITY
413
465
600
1721
1942
0
0.1
0.2
0.3
0.4
0.5
eV
0
800
1600
2400
3200
4000
cm⁻¹

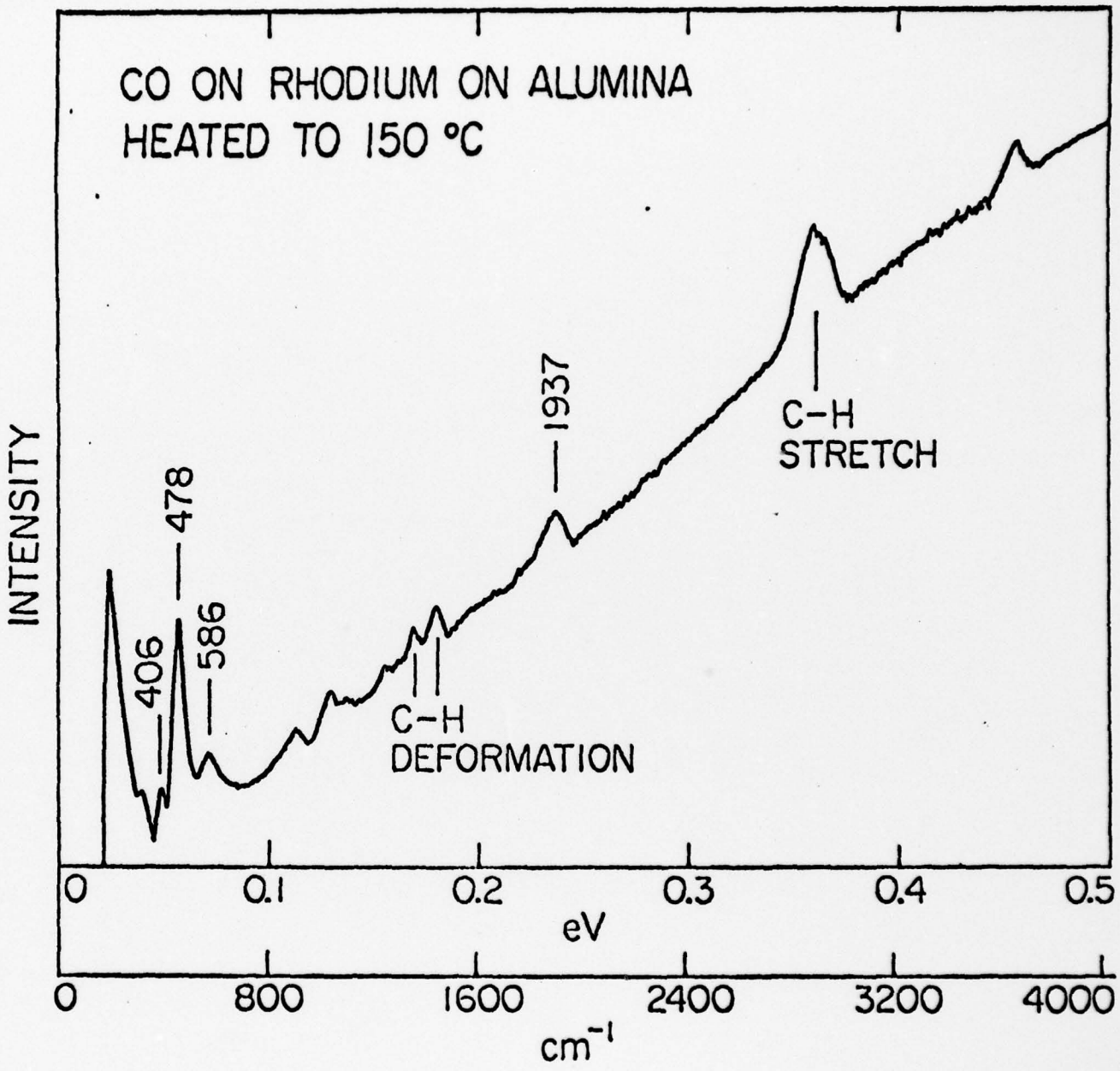
CO ON RHODIUM ON ALUMINA
HEATED TO 150 °C
INTENSITY
406
478
586
1937
C-H
DEFORMATION
C-H
STRETCH
0
0.1
0.2
0.3
0.4
0.5
eV
0
800
1600
2400
3200
4000
cm⁻¹

FIG. 3

472:GAN:716:tam
78u472-608

TECHNICAL REPORT DISTRIBUTION LIST, GEN

	No. Copies
ffice of Naval Research 00 North Quincy Street rlington, Virginia 22217 ttn: Code 472	2
NR Branch Office 36 S. Clark Street hicago, Illinois 60605 ttn: Dr. George Sandoz	1
NR Branch Office 15 Broadway ew York, New York 10003 ttn: Scientific Dept.	1
NR Branch Office 030 East Green Street asadena, California 91106 ttn: Dr. R. J. Marcus	1
NR Area Office ne Hallidie Plaza, Suite 601 an Francisco, California 94102 ttn: Dr. P. A. Miller	1
ONR Branch Office Building 114, Section D 666 Summer Street Boston, Massachusetts 02210 Attn: Dr. L. H. Peebles	1
Director, Naval Research Laboratory Washington, D.C. 20390 Attn: Code 6100	1
The Assistant Secretary of the Navy (R,E&S) Department of the Navy Room 4E736, Pentagon Washington, D.C. 20350	1
Commander, Naval Air Systems Command Department of the Navy Washington, D.C. 20360 Attn: Code 310C (H. Rosenwasser)	1

	No. Copies
Defense Documentation Center Building 5, Cameron Station Alexandria, Virginia 22314	12
U.S. Army Research Office P.O. Box 1211 Research Triangle Park, N.C. 27709 Attn: CRD-AA-IP	1
Naval Ocean Systems Center San Diego, California 92152 Attn: Mr. Joe McCartney	1
Naval Weapons Center China Lake, California 93555 Attn: Dr. A. B. Amster Chemistry Division	1
Naval Civil Engineering Laboratory Port Hueneme, California 93401 Attn: Dr. R. W. Drisko	1
Professor K. E. Woehler Department of Physics & Chemistry Naval Postgraduate School Monterey, California 93940	1
Dr. A. L. Slafkosky Scientific Advisor Commandant of the Marine Corps (Code RD-1) Washington, D.C. 20380	1
Office of Naval Research 800 N. Quincy Street Arlington, Virginia 22217 Attn: Dr. Richard S. Miller	1
Naval Ship Research and Development Center Annapolis, Maryland 21401 Attn: Dr. G. Bosmajian Applied Chemistry Division	1
Naval Ocean Systems Center San Diego, California 91232 Attn: Dr. S. Yamamoto, Marine Sciences Division	1

Encl 1

TECHNICAL REPORT DISTRIBUTION LIST, 056

	No. Copies
Dr. D. A. Vroom IRT P.O. Box 80817 San Diego, California 92138	1
Dr. G. A. Somorjai University of California Department of Chemistry Berkeley, California 94720	1
Dr. L. N. Jarvis Surface Chemistry Division 4555 Overlook Avenue, S.W. Washington, D.C. 20375	1
Dr. J. B. Hudson Rensselaer Polytechnic Institute Materials Division Troy, New York 12181	1
Dr. John T. Yates National Bureau of Standards Department of Commerce Surface Chemistry Section Washington, D.C. 20234	1
Dr. Theodore E. Madey Department of Commerce National Bureau of Standards Surface Chemistry Section Washington, D.C. 20234	1
Dr. J. M. White University of Texas Department of Chemistry Austin, Texas 78712	1
Dr. F. W. Vaughan California Institute of Technology Division of Chemistry & Chemical Engineering Pasadena, California 91125	1
Dr. Keith H. Johnson Massachusetts Institute of Technology Department of Metallurgy and Materials Science Cambridge, Massachusetts 02139	1
Dr. J. E. Demuth IBM Corportion Thomas J. Watson Research Center P.O. Box 218 Yorktown Heights, New York 10598	1
Dr. C. P. Flynn University of Illinois Department of Physics Urbana, Illinois 61801	1
Dr. W. Kohn University of California (San Diego) Department of Physics LaJolla, California 92037	1
Dr. R. L. Park Director, Center of Materials Research University of Maryland College Park, Maryland 20742	1
Dr. W. T. Peria Electrical Engineering Department University of Minnesota Minneapolis, Minnesota 55455	1
Dr. Narkis Tzoar City University of New York Convent Avenue at 138th Street New York, New York 10031	1
Dr. Chia-wei Woo Northwestern University Department of Physics Evanston, Illinois 60201	1
Dr. D. C. Mattis Yeshiva University Physics Department Amsterdam Avenue & 185th Street New York, New York 10033	1
Dr. Robert M. Hexter University of Minnesota Department of Chemistry Minneapolis, Minnesota 55455	1

472:CAN:716:tam
78u472-608

TECHNICAL REPORT DISTRIBUTION LIST, 056

	No. Copies
Dr. Leonard Wharton James Franck Institute Department of Chemistry 5640 Ellis Avenue Chicago, Illinois 60637	1
Dr. M. G. Lagally Department of Metallurgical and Mining Engineering University of Wisconsin Madison, Wisconsin 53706	1
Dr. Robert Gomer James Franck Institute Department of Chemistry 5640 Ellis Avenue Chicago, Illinois 60637	1
Dr. R. G. Wallis University of California (Irvine) Department of Physics Irvine, California 92664	1
Dr. D. Ramaker Chemistry Department George Washington University Washington, D.C. 20052	1
Dr. F. Hansma Chemistry Department University of California, Santa Barbara Santa Barbara, California 93106	1
Dr. P. Hendra Chemistry Department Southhampton University England SO9JNH	1
Professor P. Skell Chemistry Department Pennsylvania State University University Park, Pennsylvania 16802	1